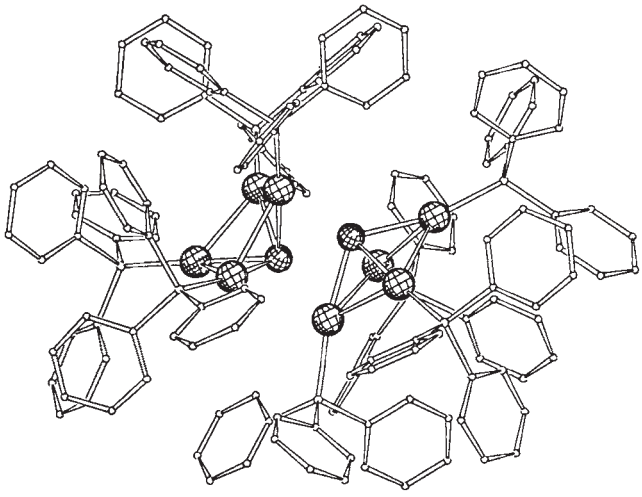

FIG. 3 Packing of two cations $[(C_6H_5)_3PAu]_4As^+$ in crystals of the tetrafluoroborate salt **2a″** (tetrafluoroborate anions and dichloromethane molecules omitted).

Against all expectations, the cations have a tetragonal pyramidal structure, with the arsenic atom occupying the apex above a slightly distorted square of gold atoms (Fig. 2). The coordination geometry at each gold atom (P–Au–As) is nearly linear, and the average apical Au–As–Au angle is 70.7° for both **2a′** and **2a″**, with an average As–Au distance of 2.50 Å (2.49 Å) and (probably the most important point) average intramolecular Au···Au contacts at 2.90 Å (2.89 Å). In the crystals, the cations appear in pairs (Fig. 3), with two longer intermolecular As···Au and Au···Au contacts in **2a′** (two Au···Au contacts in **2a″**) of 3.117 and 3.672 Å (2 × 3.414 Å), respectively. These are probably responsible for some of the structural distortions of the individual units, for the splitting of the ^{197}Au Mössbauer lines and for the colour changes. There is ample evidence, however, that these contacts are not retained in solution (colour, NMR) or in the gas phase (fast-atom-bombardment mass spectrometry). The monomers are related by C_2 and C_i point group symmetry in **2a′** and **2a″**, respectively.

There is no precedent for such an unusual structure of molecules with a tetracoordinate central atom and eight valence electrons as part of a flexible, nonforcing skeleton[20]. If only radial As–Au bonding is considered, and a lone pair of electrons is allocated to the As apex, then the $AsAu_4$ core has to be described as electron-deficient with only three bonding molecular orbitals filled under local C_{4v} symmetry. It is very likely, however, that peripheral Au···Au bonding strongly contributes to the cluster stability, as indicated by the short Au···Au distances of less than 3.00 Å at the base of the As-capped pyramid. Taking the As–Au distances of 2.50 Å as a basis, a simple calculation shows that the Au···Au contacts in an As-centred tetrahedron would be ~4.08 Å, and thus far too long for efficient Au···Au interactions[2,21]. In the nitrogen-centred tetrahedron (**1c**), on the other hand, the small atomic radius of nitrogen (as compared with arsenic) still allows Au···Au contacts of ~3.25 Å and thus makes a rearrangement to a pyramidal geometry unnecessary.

It thus seems that the concept of bonding Au···Au interactions between seemingly closed-shell ($5d^{10}$) configurations, broken up through relativistic effects ('aurophilicity'[2]), provides the solution of what otherwise could have been yet another paradox in the chemistry of metallo-complexes of gold. It has been pointed out previously[2,22,23] that many of the special features in gold chemistry have their origin in relativistic effects, which are known to be a local maximum for this element. As the velocity of the electrons in the electric field of very highly charged nuclei (such as gold, $Z = 79$) approaches the velocity of light, considerable changes in their relative energy levels arise, which reduce the gap particularly between the $6s/6p$ and 5d states, thus allowing additional bonding not foreseen in classical terms. More detailed theoretical work, already successful[22–27] for a description of the bonding in hypercoordinate carbon atoms[3–5] of the types $(LAu)_6C^{2+}$ and $(LAu)_5C^+$, is in progress. □

Received 27 February; accepted 9 May 1991.

1. Grohmann, A., Riede, J. & Schmidbaur, H. *Nature* **345,** 140–142 (1990).
2. Schmidbaur, H. *Gold. Bull.* **23,** 11–20 (1990).
3. Scherbaum, F., Grohmann, A., Huber, B., Krüger, C. & Schmidbaur, H. *Angew. Chem. Int. Edn Engl.* **27,** 1544–1546 (1988).
4. Scherbaum, F., Grohmann, A., Müller, G. & Schmidbaur, H. *Angew. Chem. Int. Edn Engl.* **28,** 463–465 (1989).
5. Scherbaum, F., Huber, B., Müller, G. & Schmidbaur, H. *Angew Chem. Int. Edn Engl.* **27,** 1542–1544 (1988).
6. Greenwood, N. N. & Earnshaw, A. N. *Chemistry of the Elements* (Pergamon, Oxford, 1986).
7. Hoffmann, R. *Angew. Chem. Int. Edn Engl.* **21,** 711–723 (1982).
8. Stone, F. G. A. *Angew. Chem. Int. Edn Engl.* **23,** 85–95 (1984).
9. Hall, K. P. & Mingos, D. M. P. *Prog. inorg. Chem.* **32,** 237–254 (1984).
10. Slovokhotov, Yu. L. & Struchkov, Yu. T. *J. organometall. Chem.* **277,** 143–146 (1984).
11. Perevalova, E. G., Smyslova, E. I., Dyadchenko, V. P., Grandberg, K. I. & Nesmeyanov, A. N. *Izv. Akad. Nauk SSSR Ser. Khim.* **1455** (1980) (in Russian).
12. Brodbeck, A. thesis, Univ. of Tübingen (1990).
13. Brodbeck, A. & Strähle, J. *Acta Crystallogr.* A**46,** C-232 (1990).
14. Kolb, A. & Bissinger, P. thesis, Techn. Univ. München (1990).
15. Grohmann, A., Riede, J. & Schmidbaur, H. *J. chem. Soc. Dalton Trans.* 783–788 (1991).
16. Ramamoorthy, V. & Sharp, P. R. *Inorg. Chem.* **29,** 3336–3340 (1990).
17. Weidenhiller, G., Steigelmann, O., Riede, J. & Schmidbaur, H. *Angew. Chem. Int. Edn Engl.* **29,** 433–435 (1991).
18. Becker, G., Gutekunst, G. & Wessely, H. J. *Z. anorg. allg. Chem.* **462,** 113–129 (1980).
19. Nesmeyanov, A. N. *et al. J. organometall. Chem.* **201,** 343–349 (1980).
20. Schmidbaur, H., Aly, A. A. M. & Schubert, U. *Angew. Chem. Int. Edn Engl.* **17,** 846–847 (1978).
21. Jones, P. G. *Gold Bull.* **19,** 46–57 (1986).
22. Rösch, N., Görling, A., Ellis, D. E. & Schmidbaur, H. *Angew. Chem. Int. Edn Engl.* **28,** 1357–1359 (1989).
23. Rösch, N., Görling, A., Ellis, D. E. & Schmidbaur, H. *Inorg. Chem.* (in the press).
24. Mingos, D. M. P. *J. Chem. Soc. Dalton Trans.* 1163–1170 (1976).
25. Evans, D. G., Mingos, D. M. P. *J. organometall. Chem.* **232,** 171–174 (1982).
26. Mingos, D. M. P. *Nature* **345,** 113–114 (1990).
27. Mingos, D. M. P. & Kanters, R. P. F. *J. organometall. Chem.* **384,** 405–415 (1990).

ACKNOWLEDGEMENTS. We thank F. E. Wagner and F. H. Kreissl for recording the Mössbauer and mass spectra, respectively. This work was supported by the Deutsche Forschungsgemeinschaft (Leibniz-Programm), the Fonds der Chemischen Industrie, and by Degussa AG and Hereaus GmbH.

Forces between polymer-bearing surfaces undergoing shear

Jacob Klein, Dvora Perahia & Sharon Warburg

Polymer Research Department, Weizmann Institute of Science, Rehovot 76100, Israel

ADSORBED or grafted polymers are used to control phenomena such as colloidal stability, fluid flow and the tribological properties of surfaces. Forces between polymer-bearing surfaces have been studied comprehensively over the past decade[1–10], but little is known about such forces in shear. These are intimately related to the dynamic as well as the equilibrium properties of the surface-attached chains. We have constructed a device that measures directly the forces that act between surfaces bearing polymer layers in a liquid medium as they slide past each other. For the case of mica sheets bearing end-grafted chains of polystyrene in toluene (a good solvent), we find that, as the surfaces move parallel to each other, there is a marked change in the normal forces between them. These become increasingly repulsive at higher velocities. The effect occurs only above certain critical shear rates, probably related to relaxation dynamics of the end-grafted chains themselves. Our findings have direct implications for the properties of polymeric lubricants, and for the rheological behaviour both of stabilized dispersions and of multi-phase polymeric systems.

Our apparatus, shown schematically in Fig. 1, can measure simultaneously both the normal forces $F_\perp(D)$ and the lateral (shear) forces $F_\parallel(D)$ between curved mica surfaces as they slide past each other a closest distance D apart. It resembles previous approaches used to investigate frictional and viscous forces

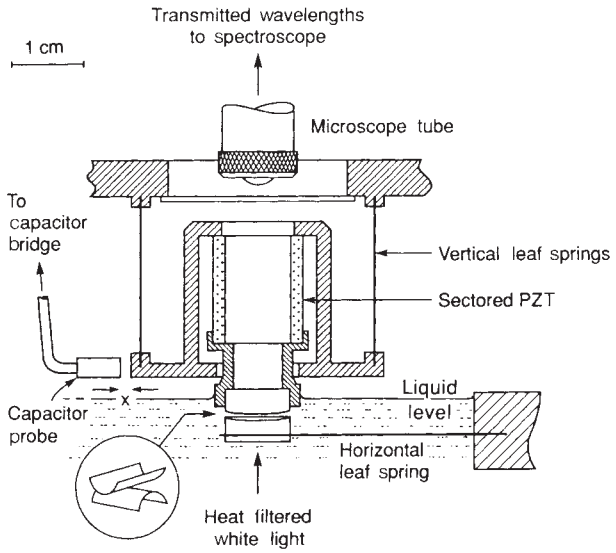

FIG. 1 Schematic diagram of measuring apparatus. The closest distance D between curved mica surfaces immersed in liquid is measured to ±0.2 nm using optical interferometry[1,17,18], and is controlled by a three-stage mechanism. The fine stage is the sectored piezoelectric tube (Vernitron PZT 8-8031-5H), mounted on vertical springs, which can move the top mica surface normally and laterally[16] (to ±0.1 nm in the x direction) relative to the lower surface. Lateral movements of up to 3 μm are possible, either monotonically, or at frequencies up to 540 Hz, or by means of a step pulse. Suitable coupling of the potential of the PZT inner surface to that of its outer sectors ensures parallel motion of the surfaces (less than 1 nm change in D over 2 μm lateral displacement). Bending of the vertical springs is monitored by an air-gap capacitor (MIA, amplifier AS-1021 PA/06, Probe ASP-1-LA) to within $\delta x = \pm 0.3$ nm. Stiffnesses K_1 and K_2 of the vertical and horizontal leaf-springs are 3.0×10^2 N m^{-1} and 1.5×10^2 N m^{-1} respectively, providing a resolution $K_1 \delta x$ of better than 10^{-7} N in measuring the lateral forces. The surfaces and lower spring are immersed in a small stainless steel bath (volume 16 ml, not shown) enclosed in a larger stainless steel box; all parts in contact with liquid are stainless steel, glass or chlorotrifluoroethylene.

between sliding mica sheets close to contact[11-15]. The present device has been designed to measure the very different effects associated with the shear of macromolecular surface phases. A sectored piezoelectric tube (PZT) is mounted on vertical leaf-springs and used to move the upper surface either laterally[16] or normally relative to the lower one which is mounted on a horizontal leaf-spring. Lateral forces between the surfaces bend the vertical springs, and this bending is measured (to within ±0.3 nm) using an air-gap capacitor. Normal forces between them are monitored through the bending of the horizontal spring, using optical interferometry as in earlier studies[1-5,17,18]. Extremely parallel motion of the surfaces over a wide range of velocities is possible using the sectored PZT; in particular, this allows us to measure the coupling between shear and normal forces. Overall, we can measure normal and lateral forces with comparable resolution and sensitivity.

Normal forces $F_\perp(D)$ between the curved mica sheets without shearing were measured as described in earlier studies[4,5], both before and after coverage of the surfaces by polymeric chains from the surrounding toluene medium. The range and magnitude of these forces (Fig. 2*a*) are closely similar to values earlier reported, and reveal unambiguously the tethering of the polymer to the mica surface by the zwitterion at its end[4,5]. Such profiles, which also indicate the amount of polymer on each surface,

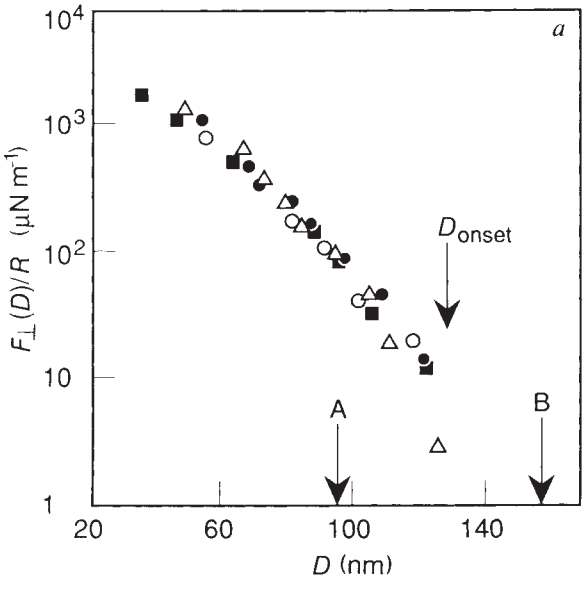

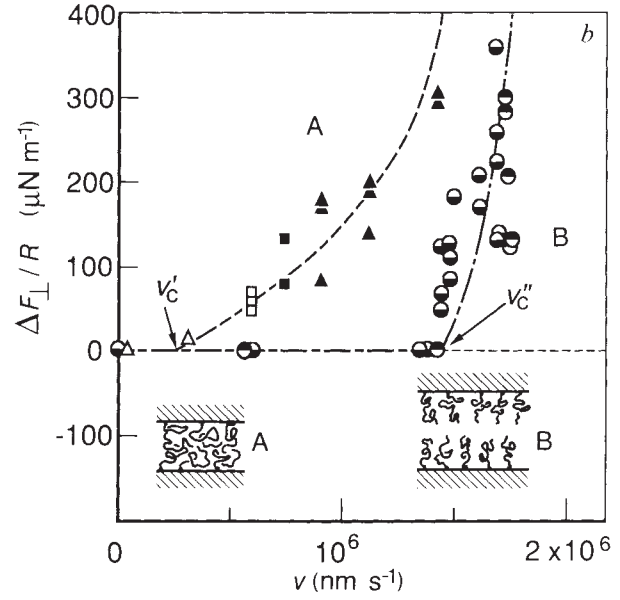

FIG. 2 *a*, Normal force profile $F_\perp(D)/R$ between curved mica sheets (mean radius of curvature $R \approx 1$ cm) a closest distance D apart. Sucrose was used to glue the sheets to the glass formers. The surfaces are immersed in a solution 0.01 wt% of zwitterion-terminated polystyrene, PS-X, in toluene (Fluka, spectroscopic grade) at 23 ± 1 °C and are covered by layers of the polymer, anchored to each surface by the zwitterion group $(N^+(CH_3)_2(CH_2)_3SO_3^-)$. Different symbols are from measurements carried out before and after shear of the surfaces. $D_{onset} = 125 \pm 5$ nm indicates the surface separation for onset of monotonic repulsion (the separation at which the layers come into contact), and A and B indicate the separations at which the data of Fig. 2*b* were taken. The PS-X has[2] a weight-average molecular weight 1.41×10^5 and polydispersity 1.02. *b*, Variation of the increment $\Delta F_\perp/R$ in the normal force between mica surfaces a fixed distance D apart, bearing terminally anchored PS-X layers, as a function of their mean lateral velocity v. Curves A and B are for $D = 94.5 \pm 1$ nm and $D = 155.2 \pm 1$ nm respectively, corresponding to the separations A and B indicated in Fig. 2*a*. The lateral motion is sinusoidal with frequency ν and amplitude Δx, and the velocity is evaluated as $v = 2\nu\Delta x$. In curve A, Δ is for $\nu = 200$ Hz; ▲, □ for $\nu = 400$ Hz; ■ for $\nu = 500$ Hz. In curve B, ◒ and ◓ are both at $\nu = 400$ Hz, from different runs. The continuous broken curves are a guide to the eye. The drawings (bottom) indicate schematically the polymer layers at the separations A and B when the surfaces are at rest ($v = 0$).

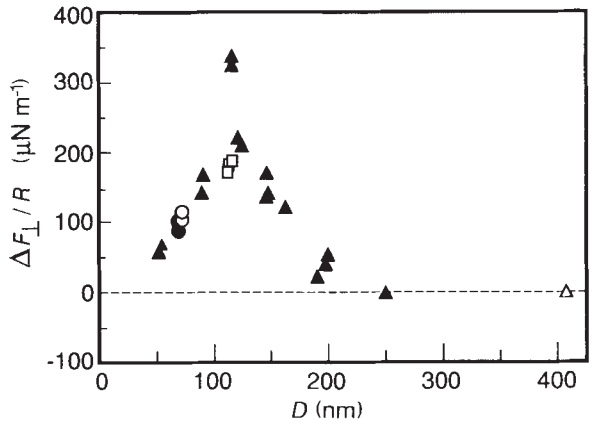

FIG. 3 Variation of the normal force increment $\Delta F_\perp/R$ at a fixed value of the mean shear velocity between mica surfaces bearing the terminally-anchored PS-X chains, as a function of their separation, D. Different symbols correspond to different runs. The motion is provided by a periodic step-pulse (half-rise time $t_{1/2}=6\times10^{-5}$ s) of amplitude $\Delta x=315$ nm, which may be considered to correspond to a mean velocity $v=\Delta x/2t_{1/2}=2.6\times10^{6}$ nm^{-1}. Because of the different waveforms (step pulse and sinusoidal, respectively) used to generate the lateral motion, it is not appropriate to compare this mean shear velocity directly with those in Fig. 2*b*.

were frequently determined during an experiment to check the integrity of the grafted layers, especially after shear. They are identical within scatter to the pre-shear profile, and indicate that shear in these experiments does not remove polymer from the anchoring mica substrates.

We investigated the effect on the normal forces $F_\perp(D)$ of sliding the top mica surface relative to the bottom one as a function of D and of the relative sliding (or shear) velocity v. For the bare mica surfaces in toluene, no change in $F_\perp(D)$ was detected down to surface separations of ~5 nm (at which point the surfaces jumped into strong adhesive contact[4]) over the entire accessible range of shear frequencies and velocities (see Fig. 1). In contrast, following the anchoring of polystyrene chains on each mica surface, we observe considerable coupling between the lateral motion and the normal forces $F_\perp(D)$ between the polymer-bearing surfaces. The horizontal spring (stiffness K_2) supporting the lower mica surface bends by ΔD when the upper surface moves at sufficiently high velocity parallel to it. Such a bending reflects a change $\Delta F_\perp = K_2\Delta D$ in the normal force acting between the surfaces.

The coupling is clearly seen in Fig. 2*b*. As v increases, little change is observed up to a certain critical velocity (marked v_c', v_c'' for the two values of D shown in Fig. 2), beyond which the additional repulsion $\Delta F_\perp$ grows rapidly; this behaviour is reversible on changing v. The increase in repulsion beyond the critical shear velocities seems to be due to lateral stretching of the surface-tethered polymer chains when they shear sufficiently rapidly past each other. At low shear velocities and moderate compressions (as for the left-hand curve in Fig. 2*b*), little lateral force $F_\parallel(D)$ is measurable between the polymer-bearing surfaces (J. K. and D. P., manuscript in preparation); once the shear rates exceed the relaxation rate of a tethered chain or of a part of it, however, there is an increased tendency to stretch it laterally. Such stretching of chains in the compressed layers is expected to increase the extent to which monomers in the gap interact and repel each other[19,20]. This in turn increases the local osmotic pressure[20] and is manifested as an increase in $\Delta F_\perp$.

Repulsion sets in suddenly at the surface separation $D=$ 155 nm (right-hand curve in Fig. 2*b*). This separation is considerably greater than the separation $D_{onset}=125$ nm for contact between the polymer layers (Fig. 2*a*), so that at rest, a substantial fluid gap separates them as indicated. The sudden increase in $\Delta F_\perp$ in this case (and in others, not shown, for which $D>D_{onset}$) suggests the following: when fluid flows rapidly enough ($v>v_c''$) past the polymer layers, it stretches the end-tethered chains, and the layers become thicker as a result (calculations by J-L. Barrat, personal communication). This thickening narrows the gap between them and increases the effective shear rate of the liquid in the gap, which leads to further thickening of the two polymer layers, and so on. This cooperative effect rapidly results in contact between the opposing layers, and their mutual repulsion, because of monomeric interactions[2], causes the sharp rise in $\Delta F_\perp$.

The variation of $\Delta F_\perp$ with surface separation D at a fixed value of the mean relative velocity v is shown in Fig. 3. At large separations ($\gtrsim$200 nm) there is no measurable repulsion between the surfaces, but as D decreases, an increasing repulsive force $\Delta F_\perp$ is induced by the shearing motion, as described above. $\Delta F_\perp$ goes through a maximum (close to $D=D_{onset}$) before decaying as the layers are progressively compressed. This behaviour is reversible on changing D, and the maximum in $\Delta F_\perp$ is found also at other (sufficiently high) shear velocities. This maximum in $\Delta F_\perp$ as the surfaces approach is due to interplay of several factors but may be qualitatively understood as follows: at large separations the shear rate in the gap is low, and any stretching of chains is not sufficient to lead to thickening of and repulsion between the layers. At lower separations ($D\leqslant$ 200 nm for the relative shear velocity in Fig. 3) such repulsion, manifested as $\Delta F_\perp$, does take place and increases as D decreases, as does the effective shear rate in the gap (as in Fig. 2*b*). At still higher compressions ($D\leqslant D_{onset}$), the increasing monomer concentration in the gap reduces the efficiency of the chain-stretching in promoting repulsive monomeric interactions[20]. This leads eventually to the observed reduction in the repulsion $\Delta F_\perp$.

Our results show that the normal forces between surfaces bearing grafted polymer layers in a good solvent increase markedly when the compressed layers are sheared, and that an uncompressed layer increases its thickness when fluid flows past it. These effects occur above certain critical shear rates, probably related to relaxation rates of the end-tethered chains. They may provide a new approach for studying the dynamic behaviour of confined macromolecules. □

Received 4 April; accepted 24 May 1991.

1. Klein, J. *Nature* **288,** 248–250 (1980).
2. Klein, J. *Molecular Conformation and Dynamics of Macromolecules in Condensed Systems* (ed. Nagasawa, M.) 333–352 (Elsevier, Amsterdam, 1988).
3. Patel, S. & Tirrell, M. *Ann. Rev. phys. Chem.* **40,** 597–635 (1989).
4. Taunton, H. J., Toprakcioglu, C., Fetters, L. J. & Klein, J. *Nature* **332,** 712–714 (1988).
5. Taunton, H. J., Toprakcioglu, C., Fetters, L. J. & Klein, J. *Macromolecules* **23,** 580–589 (1990).
6. de Gennes, P. G. *Macromolecules* **15,** 492–501 (1982).
7. Klein, J. & Pincus, P. *Macromolecules* **15,** 1129–1137 (1982).
8. Scheutjens, J. & Fleer, G. *Macromolecules* **18,** 1882–1894 (1985).
9. Alexander, S. *J. Phys.* **38,** 983–989 (1977).
10. De Gennes, P. G. *Adv. Colloid Interf. Sci.* **27,** 189–207 (1987).
11. Bailey, A. I. *J. appl. Phys.* **32,** 1407–1413 (1961).
12. Israelachvili, J. N. & Tabor, D. *Wear* **24,** 386–390 (1973).
13. Briscoe, B. J. & Evans, D. C. B. *Proc. R. Soc. Lond.* A**380,** 389–398 (1982).
14. van Alsten, J. & Granick, S. *Phys. Rev. Lett.* **61,** 2570–2573 (1988).
15. Homola, A. M. Israelachvili, J. N., Gee, M. L. & McGuiggan, P. M. *J. Tribology* **111,** 675–682 (1989).
16. Carr, R. G. *J. Microsc.* **152,** 379–388 (1988).
17. Tabor, D. & Winterton, R. H. S. *Proc. R. Soc. Lond.* A**312,** 435–450 (1969).
18. Israelachvili, J. N. & Adams, G. *J. Chem. Soc. Faraday* I **74,** 974–1001 (1978).
19. Pincus, P. *Macromolecules* **9,** 386–392 (1976).
20. Rabin, Y. & Alexander, S. *Europhys. Lett.* **13,** 49–54 (1990).

ACKNOWLEDGEMENTS. J. K. thanks C. Quate and E. J. Kramer for their suggestions. We thank L. J. Fetters for the PS-X' polymer, and R. deRoos and Y. Gat for technical assistance. We appreciate discussions with S. Alexander, J-L. Barrat, Y. Rabin, A. Silberberg and particularly F. Pincus. This work was supported by the Minerva Foundation, the National Council for Research and Development (Israel) and the Forschungszentrum Juelich (GMBH). J.H. is the incumbent of the Herman Mark chair of Polymer Physics.